SOTERIA

EFFECTS OF HELIUM ON IASCC SUSCEPTIBILITY

J. Chen
Department of nuclear energy and safety
Paul Scherrer Institute

PAUL SCHERRER INSTITUT

This project received funding under the Euratom research and training programme 2014-2018 under grant agreement N° 661913

Contributors

- Ignasi Villacampa(PSI)
- J. Chen, (PSI)
- P. Spätig (PSI)
- H.P. Seifert (PSI)
- M.F. Barthe (CEMHTI/CNRS)
- Cyclotron operator team (CEMHTI/CNRS)

Contents

What is IASCC?

By definition: IASCC is actually inter-granular SCC assisted by irradiation

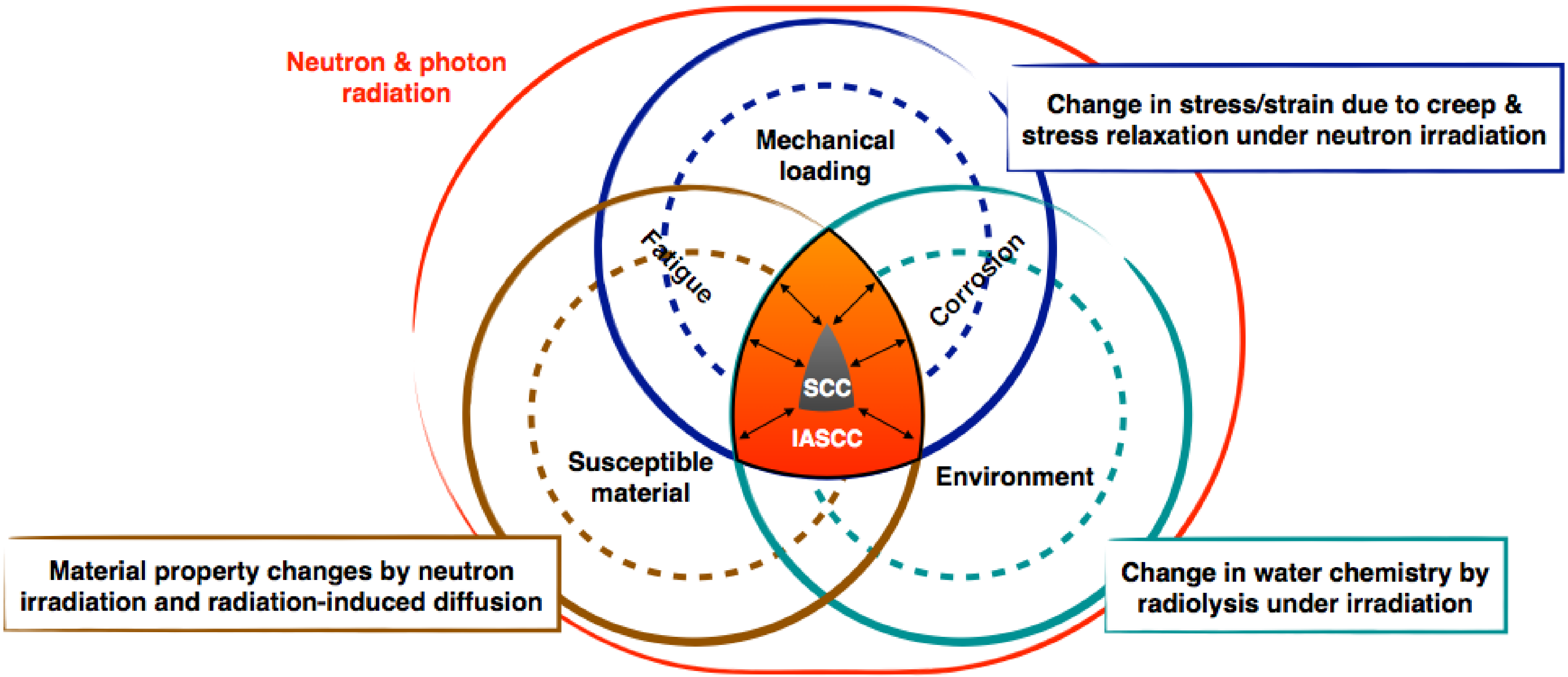

The susceptibility to SCC increase with irradiation

How is SCC measured?

Constant load

To smooth samples

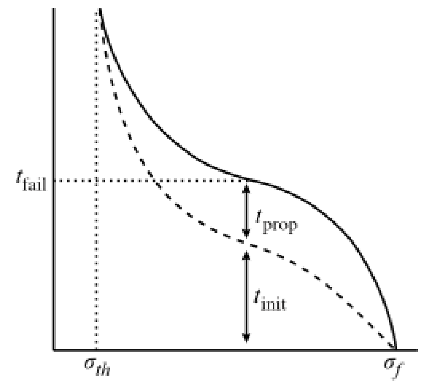

Measure the time to failure as a function of the applied stress.

To pre-cracked samples

Measure the crack length as a function of time. CGR in function of K.

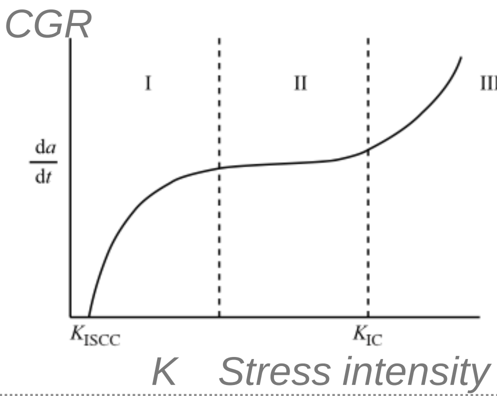

SSRT

Smooth or pre-cracked

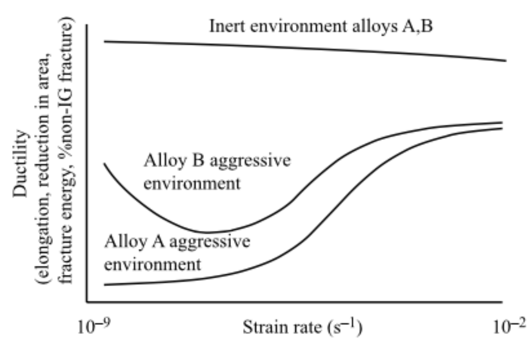

Measure of elongation, reduction of area (ductility) and TG/IG fracture.

SCC morphology (316 AuSS)

IG **TG**

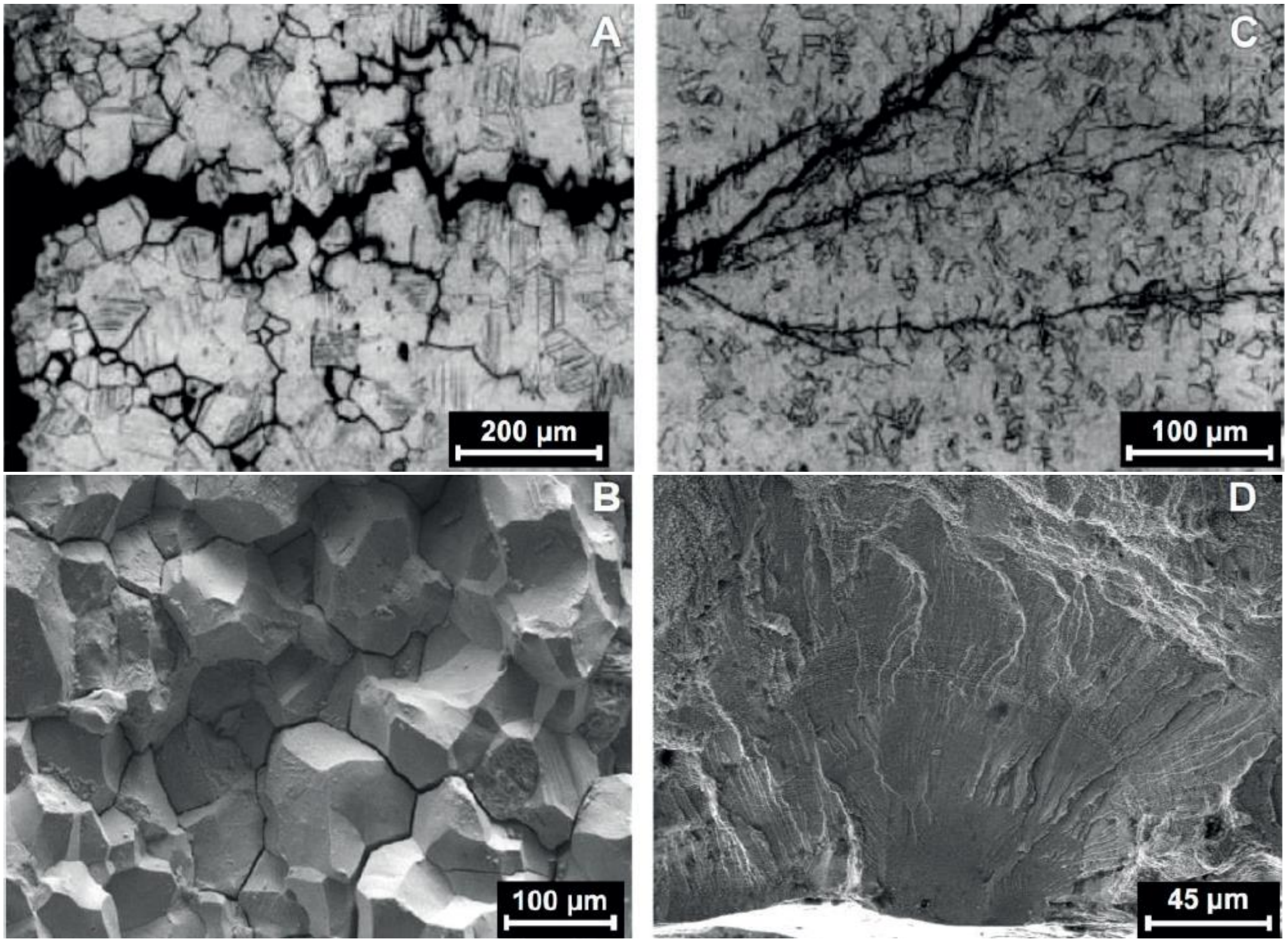

D. Landolt (2007)

D. Du et.al JNM456 (2015) 228

Cavities in the BFBs Tihange 1

Cold worked 316SS **after service in PWR** conditions

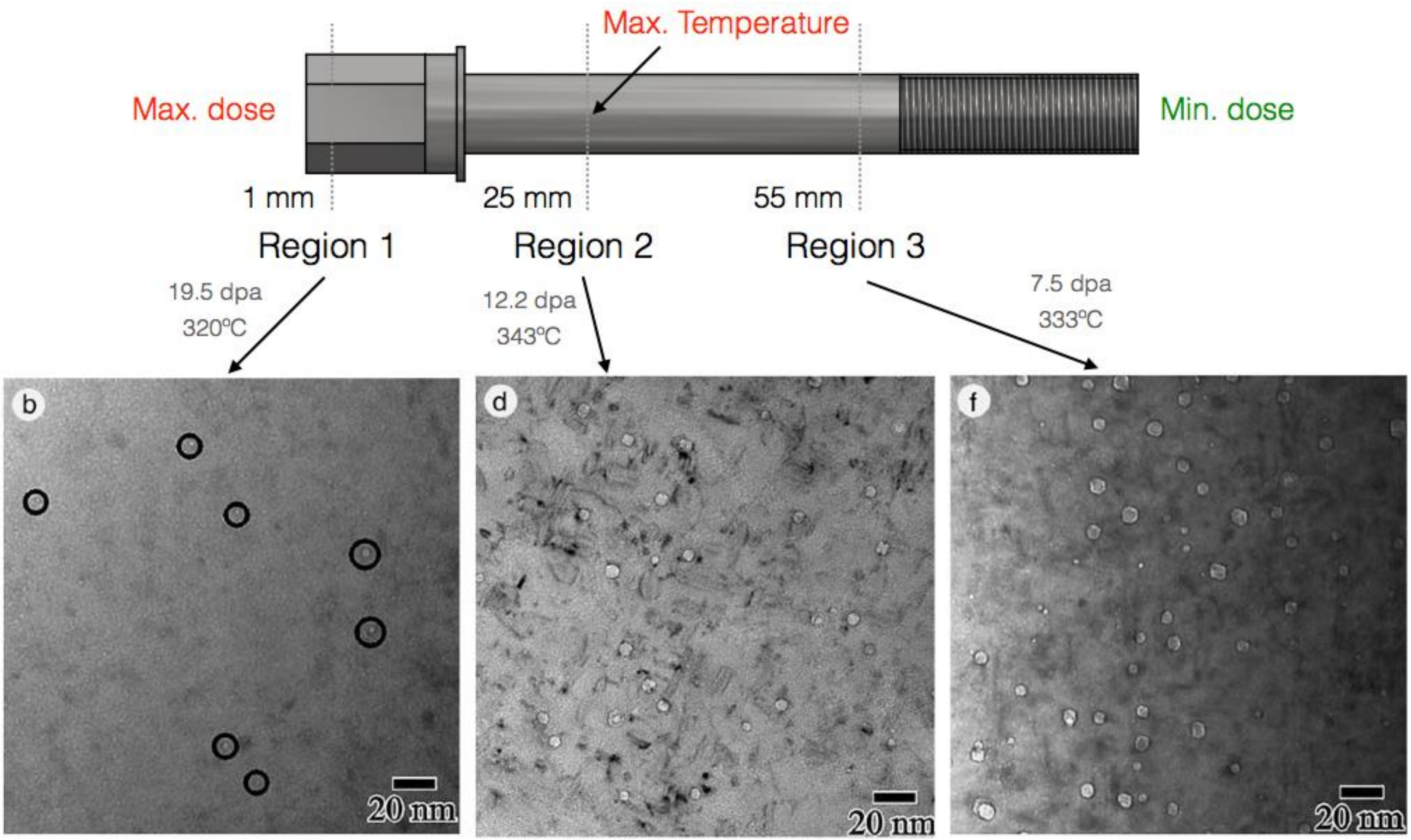

Helium & IASCC

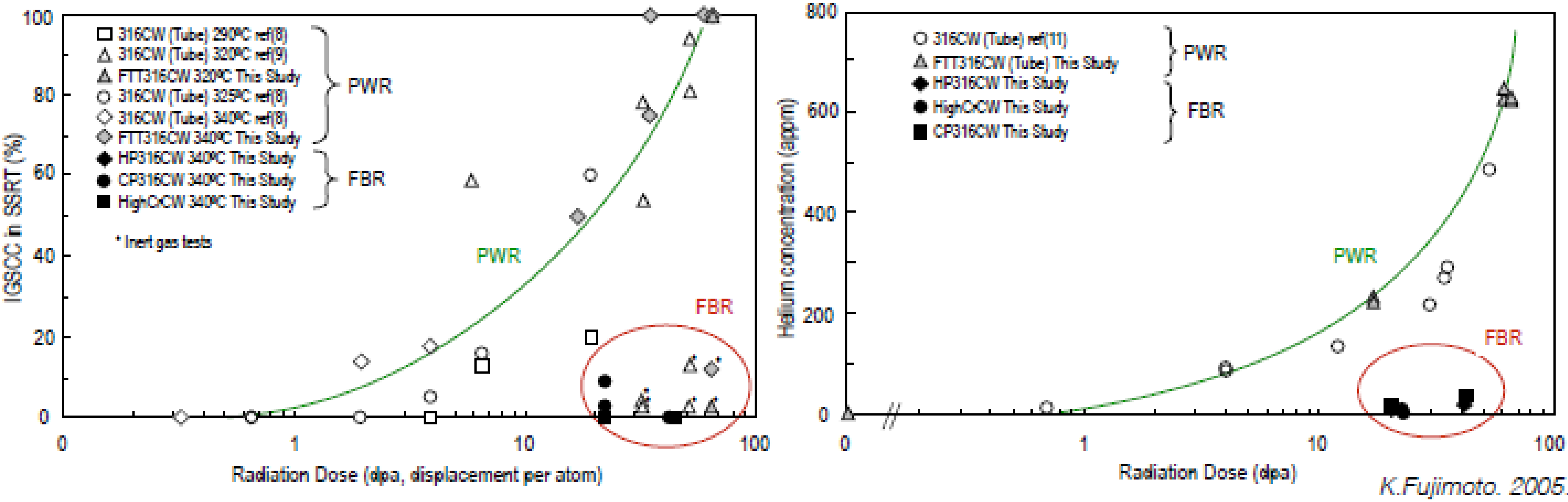

Good correlation between IGSCC susceptibility & He concentration evolution

- For given dpa, FBR-irradiated SS show much lower IASCC susceptibility than PWR-irradiated SS in spite of similar irradiation hardening and GB segregation
- He effect might be one of the main reasons for this large difference

PWR ~ 10 appm He/dpa >> FBR ~ 0.1 appm He/dpa

Selected studies on helium effects

Artificially implanted HELIUM

Tested in vacuum

SINGLE GB

>20’000 appm He

Bubble spacing < 5 nm

GB coverage = 7 %

0.95 dpa

IG fracture

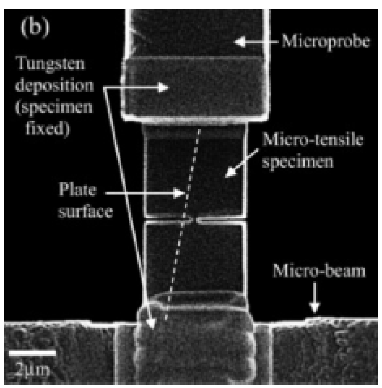

T. Miura et al., 2015.

POLYCRYSTAL*

>10’000 appm He

1 dpa

TG-C

H. Ullmaier, 2003

Irradiated in Halden reactor (BWR) 300°C

TEST IN HWC	TEST IN NWC
~few tenths appm He	~few tenths appm He
~1 dpa	>0.45-5 dpa
TG-C (<2%) + TG-D	IG (3-30%) + TG-D

Irradiated in BOR-60 (FBR) 320°C

TEST IN HWC	TEST IN NWC
~0 appm He	~0 appm He
~48 dpa	~5 dpa
TG-C (<2%) + TG-D	IG (0-50%) + TG-D

NO IG→ ↓ HE ?

Y. Chen et al., 2014

Approach

- Potential concern for some PWR internals & LTO > 50 a
- SA (baffle formers) and CW SS (baffle bolts)
- Separation of He and displacement damage effects

  → He implantation (100 to 1000 appm, 0.016 to 0.16 dpa only)
- Simulation of He bubble structure in baffle bolts & variation of He bubble size and GB He bubble coverage

  → post implantation annealing study

  → critical He concentrations or GB coverage for IG (IA)SCC
- Characterization of IG (IASCC) susceptibility by SSRT tests with smooth sample in hydrogenated HTW

  → fracture & deformation mode by SEM & TEM

Contents

Methodology – Materials & sample

316 L

Cr	Ni	Mo	Mn	Si	Co	N	V	C	P	W	Al	Ti	Sn	Nb	S
17.61	12.32	2.379	1.768	0.466	0.164	0.0673	0.036	0.0275	0.024	0.023	0.018	0.007	0.006	0.003	<0.003

- **SA at 1050ºC for 30' quenched in water**

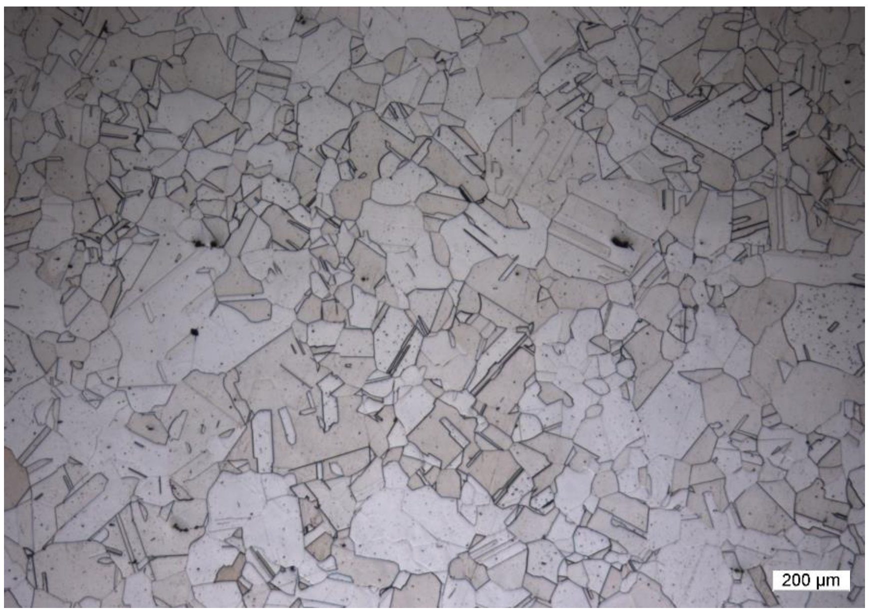

average grain size 52 µm

- **Tensile specimens** (ASTM standard)

45 MeV ≃ 250 µm

$$\frac{t_c}{s} = 7$$

$$\frac{t}{w} \geq 0.2$$

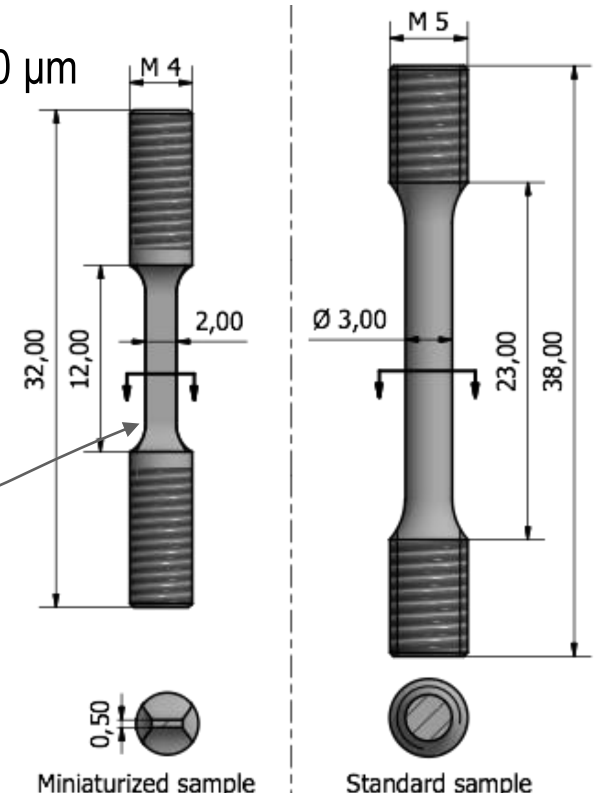

Methodology - Helium implantation

Irradiation parameters

α energy = 45 MeV
T-Irradiation = 300 °C
Fluence = 2.17 x 1018 He cm^{-2}
He-concentrations = 100, 300, 1000 appm
damage = 0.016, 0.05, 0.16 dpa

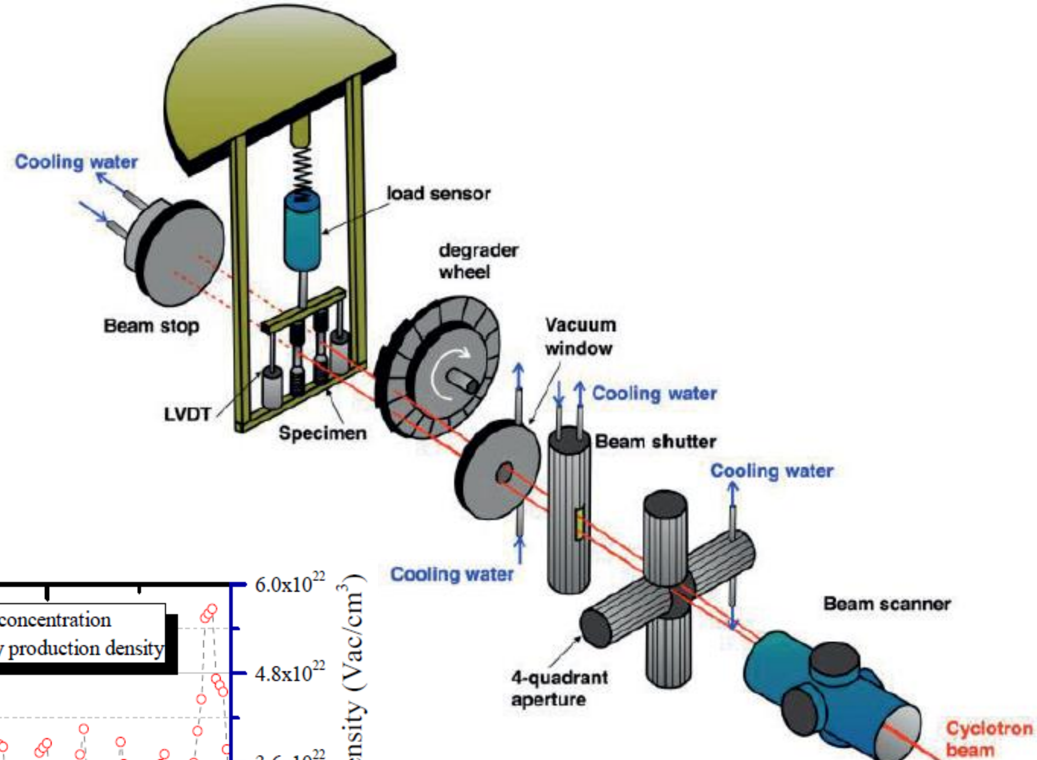

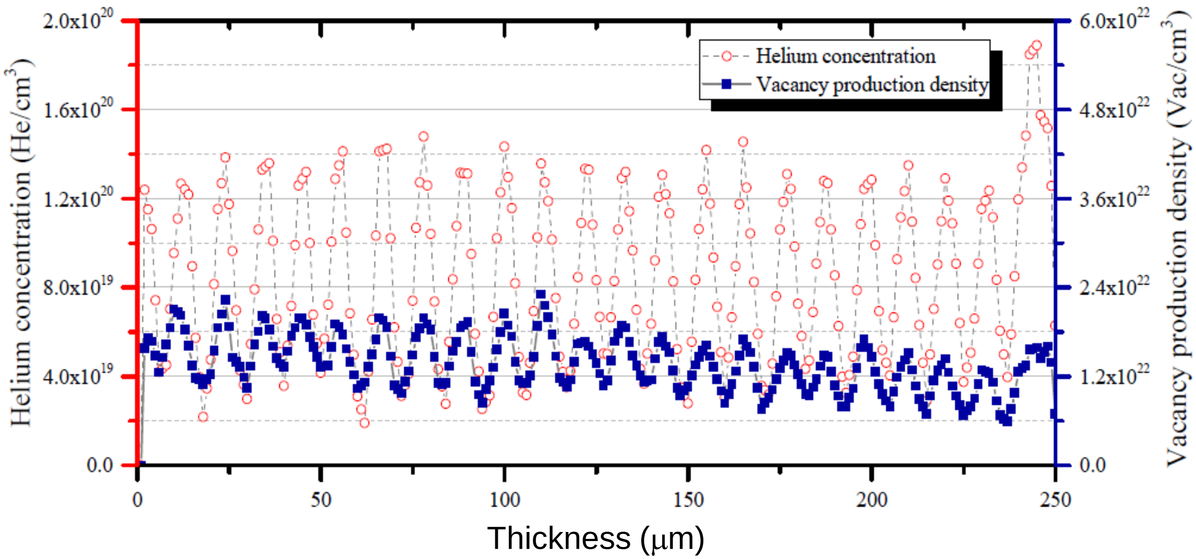

Methodology - Post implantation annealing

Objective: Reproduce BFB microstructure & increase GB coverage

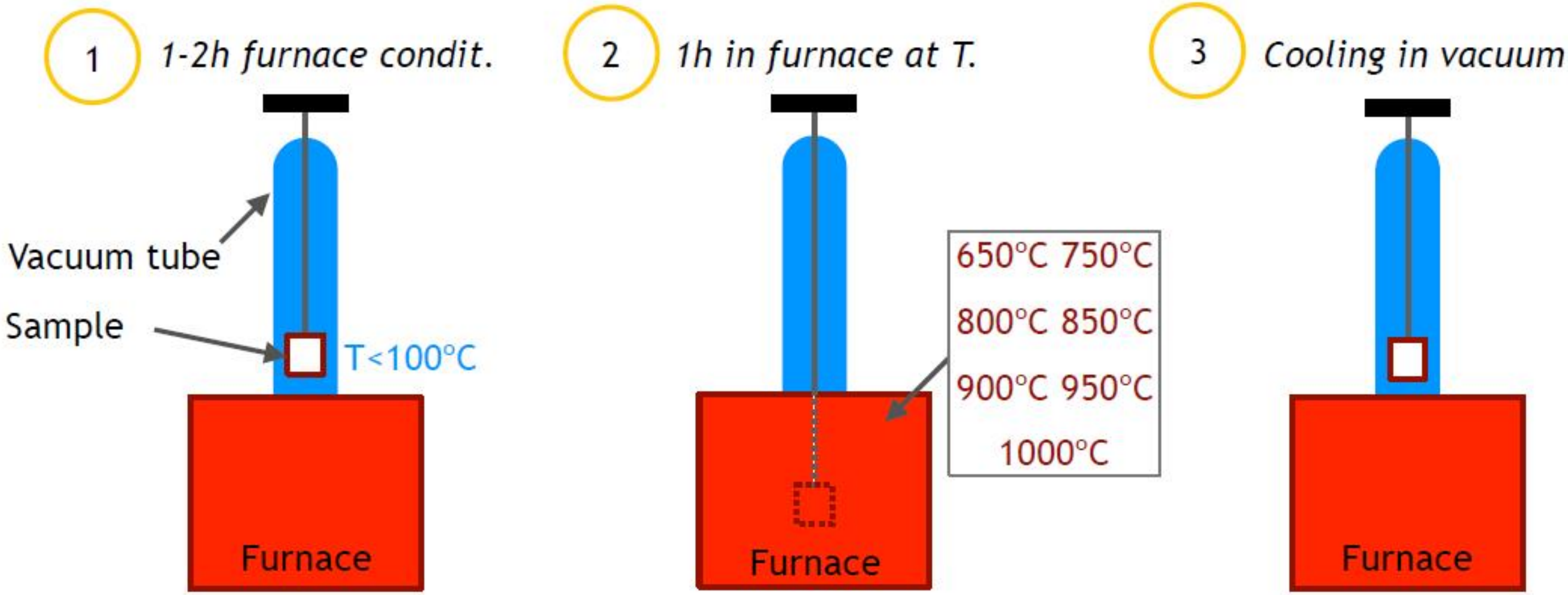

Used for He implanted **plates** and miniaturised **samples**

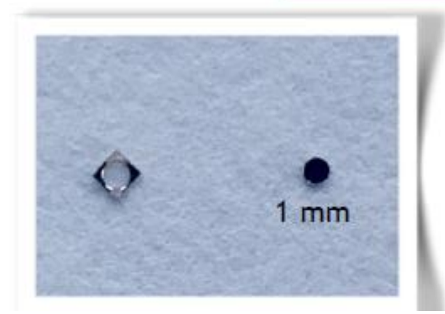

Methodology - Mechanical testing

Water loop Diagram

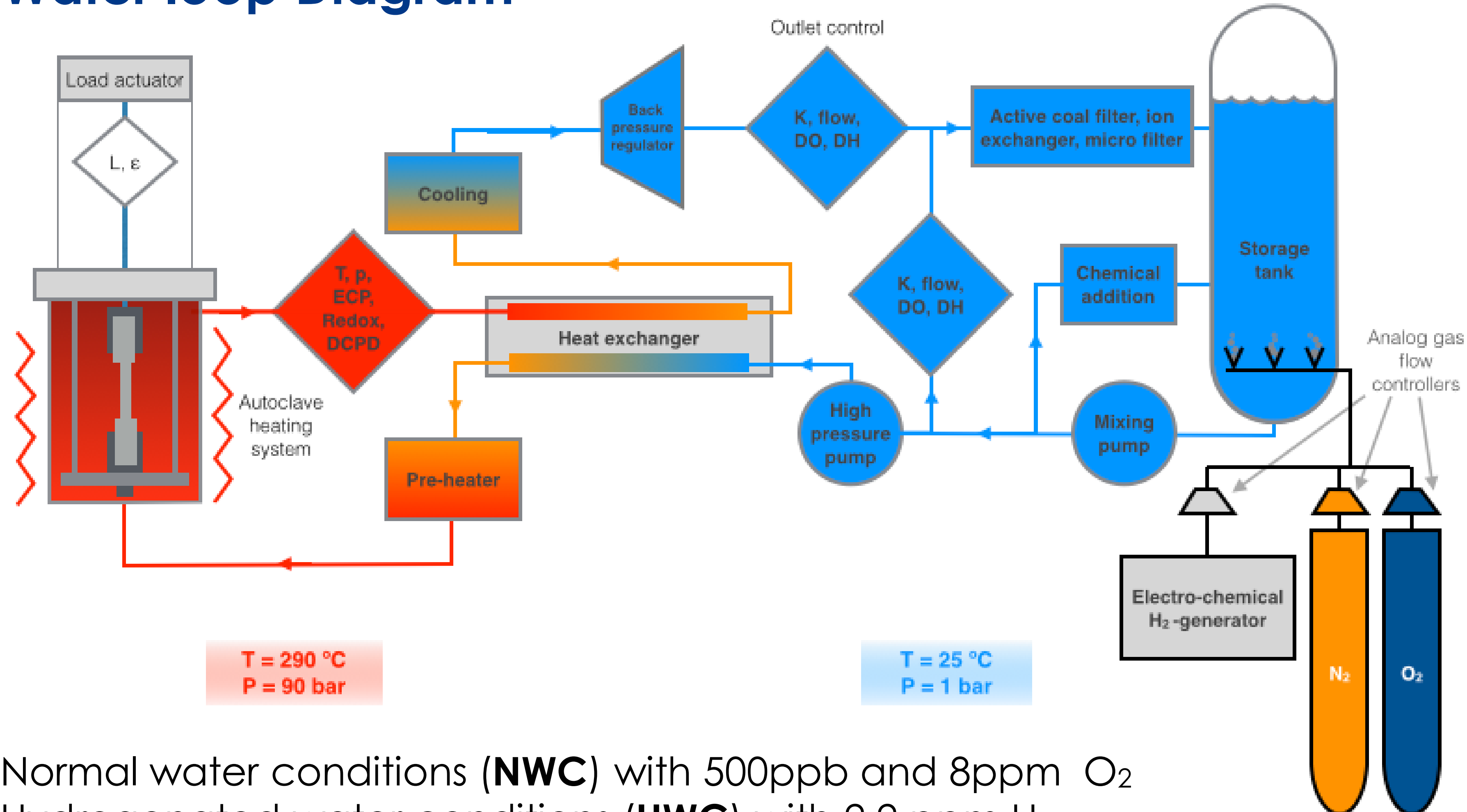

Normal water conditions (**NWC**) with 500ppb and 8ppm O_2
Hydrogenated water conditions (**HWC**) with 2.2 ppm H_2

Methodology - Mechanical testing

Water loop device located at Hot lab at PSI

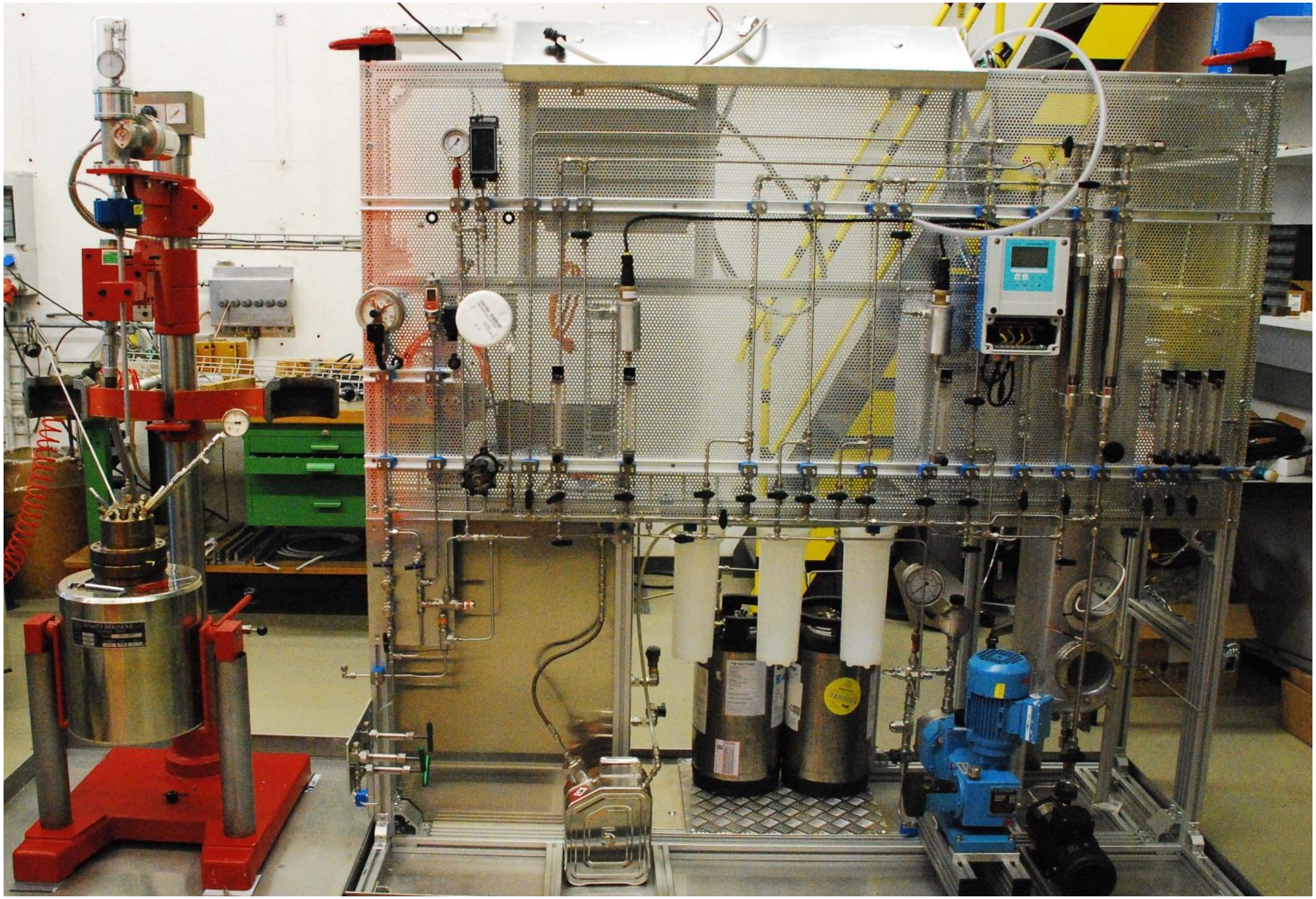

Contents

Representative engineering stress-strain curves

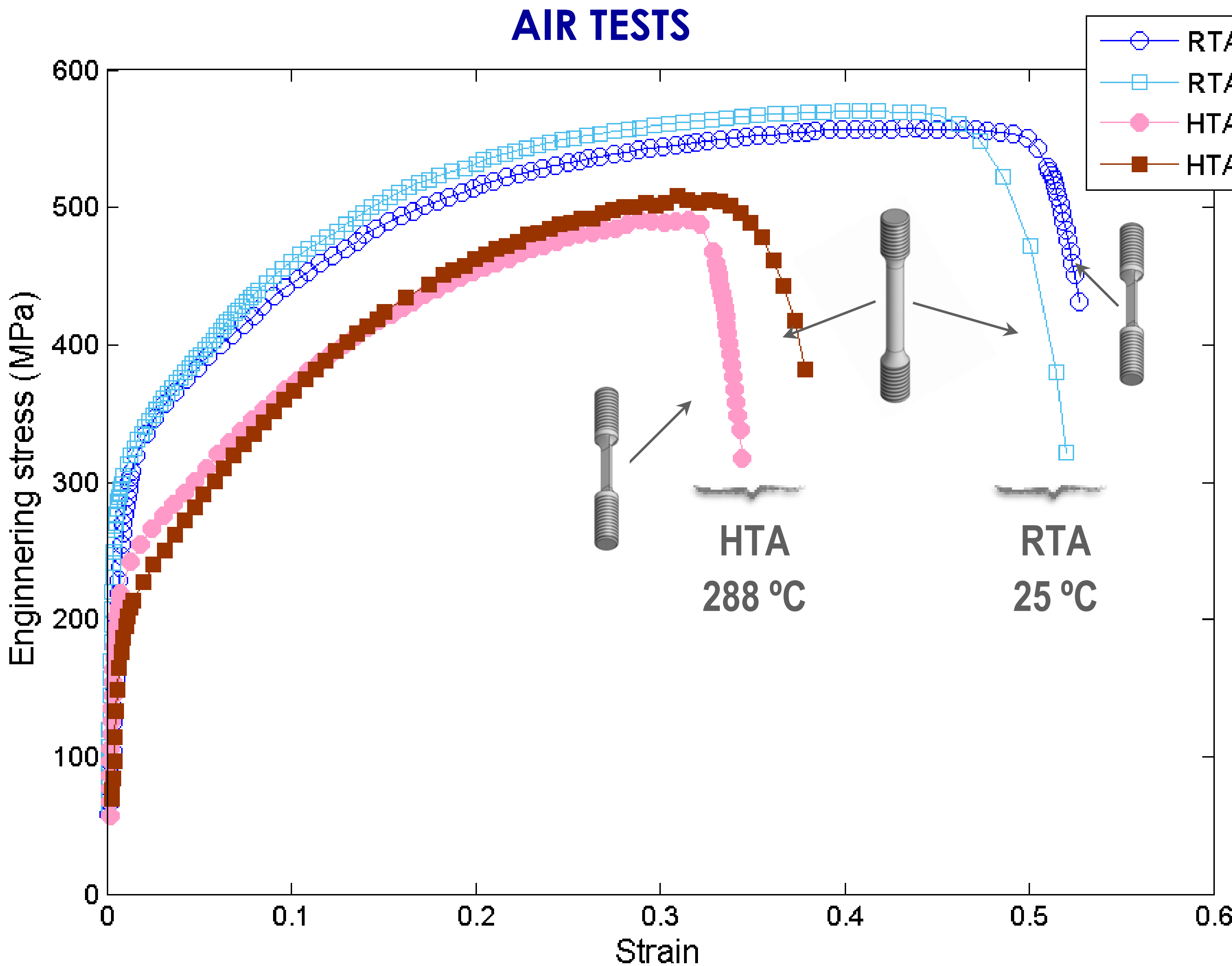

Different tensile machines

Effective gauge length

For all conditions, similar YS, UTS & US

Overview of engineering stress-strain results

Sample type	Temperature (ºC)	Environment	$Rp_{0.2\%}$ (MPa)	UTS (MPa)	US	RA
Miniaturised (5)	25	RTA	281	558	0.41	0.82
Standard (4)	25	RTA	290	577	0.41	0.83
	REL. ERROR RTA		3.0%	3.3%	0.85%	1.42%
Miniaturised (7)	288	HTA	216	500	0.29	0.79
Standard (5)	288	HTA	204	509	0.32	0.70
	REL. ERROR HTA		5.9%	1.7%	8.2%	12%
Miniaturised (1)	288	NWC (500 ppb O_2)	224	499	0.34	0.71
Standard (1)	288	NWC (500 ppb O_2)	208	527	0.38	0.68
	REL. ERROR NWC 500 ppb O_2		7.8%	5.4%	8.9%	5.1%
Miniaturised (2)	288	HWC (2.2 ppm H_2)	-	478	0.32	0.67
Standard (2)	288	HWC (2.2 ppm H_2)	234	501	0.29	0.51
	REL. ERROR HWC		-%	4.6%	11%	30%
Miniaturised (1)	288	NWC (8 ppm O_2)	192	498.8	0.29	0.72
Standard (2-3)	288	NWC (8 ppm O_2)	203	512	0.38	0.67
	REL. ERROR NWC 8 ppm O_2		5.3%	2.6%	24%	6.4%

standard and miniaturized flat dog-bone samples are almost identical !

Fracture surface

Miniaturized sample

Standard sample

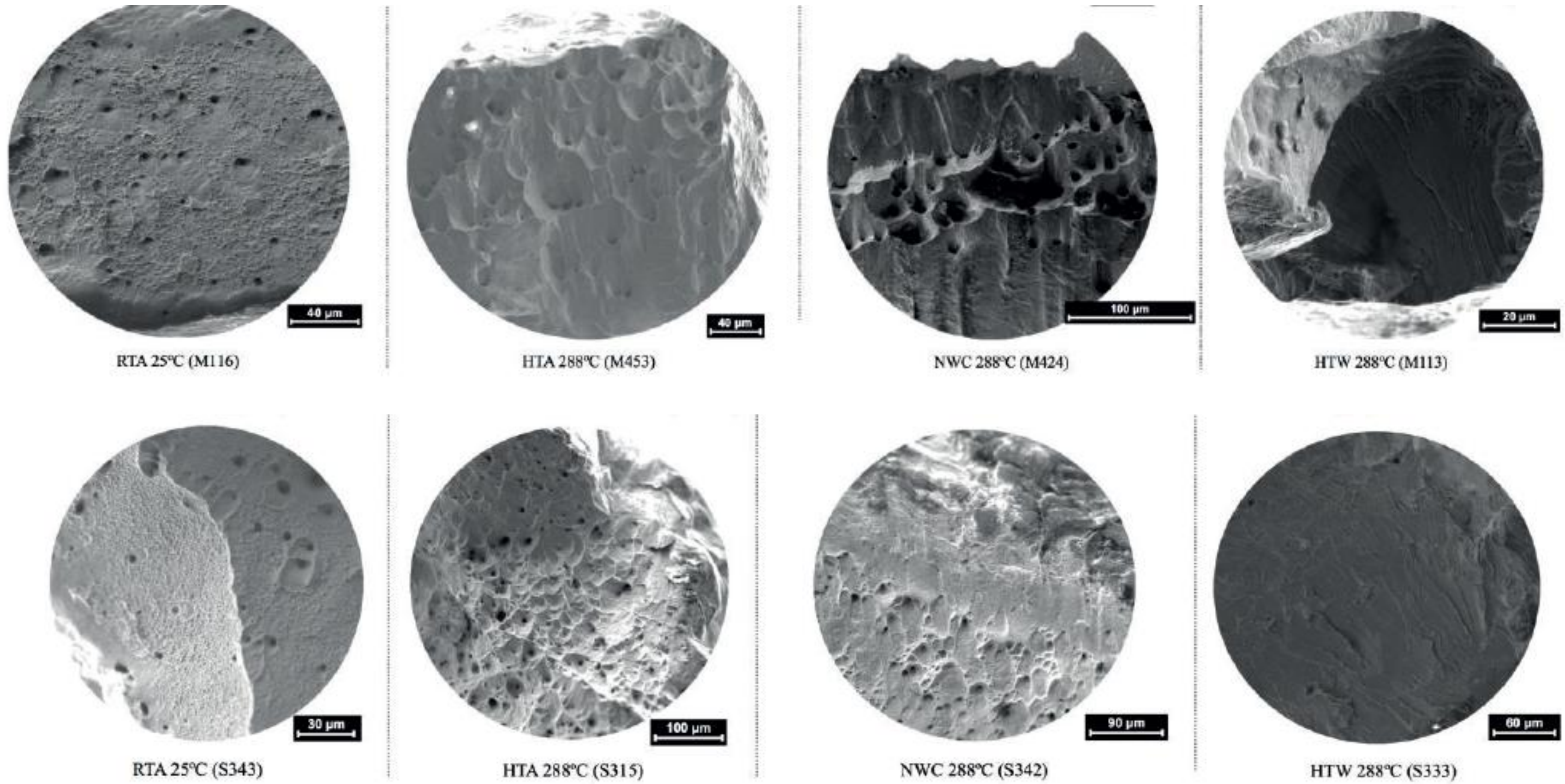

RTA 25ºC (S343)

HTA 288ºC (S315)

NWC 288ºC (S342)

HWC 288ºC (S333)

TG-D fracture

TG-D & TG-C fracture (< 3%)

Metallography investigation

Axial cuts

Standard sample

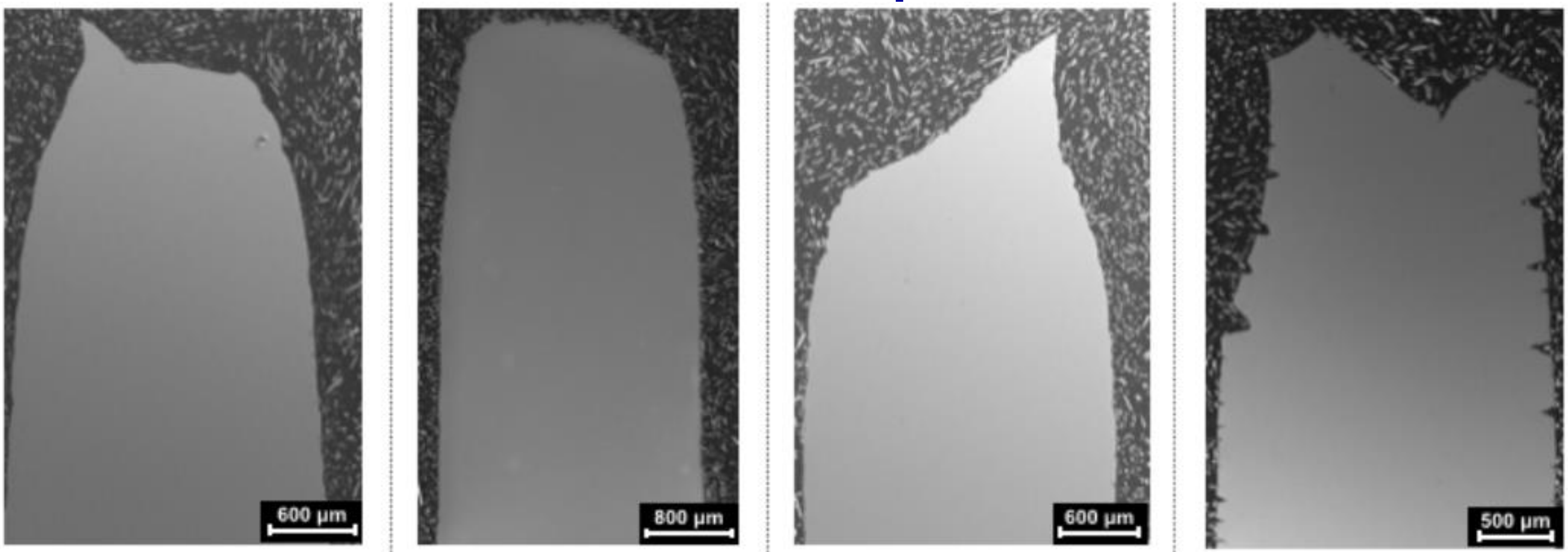

RTA 25ºC (S343) | HTA 288ºC (S315) | NWC 288ºC (S342) | HWC 288ºC (S333)

Increasing temperature → *Decrease the reduction of area*

No oxygen effect

Hydrogen effect → *Cracks initiating in the sample surface*

05/04/2018

Contents

Bubble distribution after PIA (1000 appm)

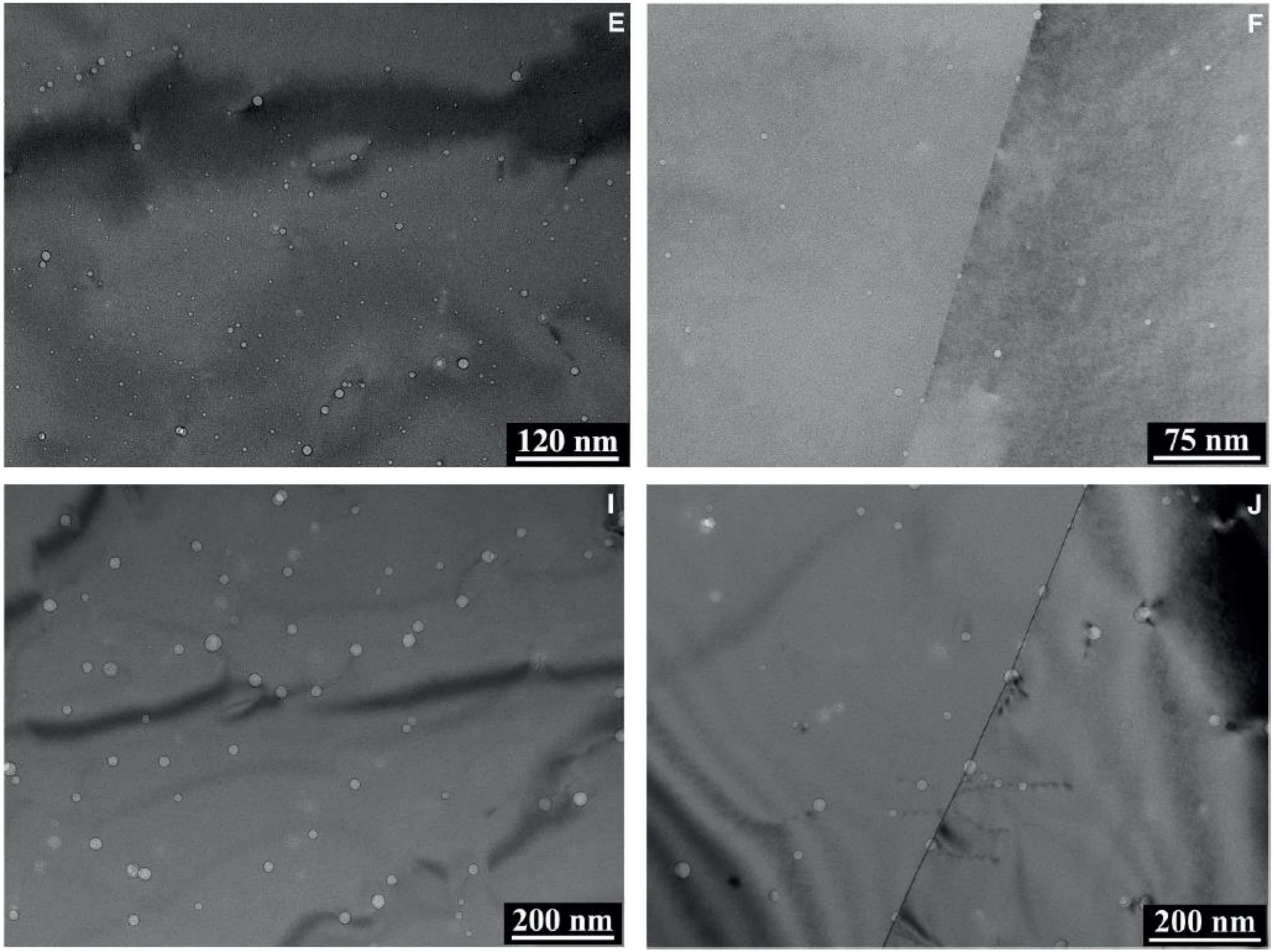

at 750°C

at 900°C

Bubble average spacing and GB coverage

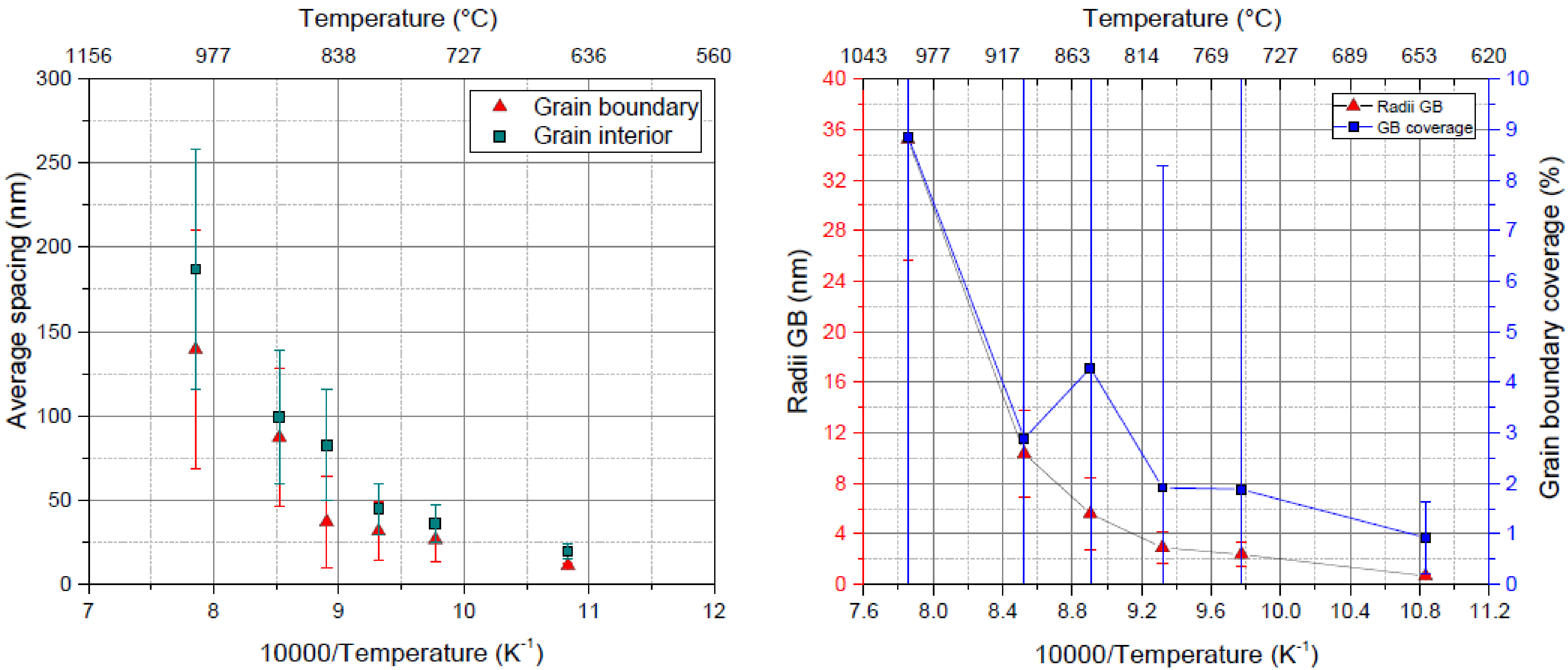

Limited of GB coverage, hence limited GB weakening

Bubble growth mechanism during PIA

Migration & Coalescence

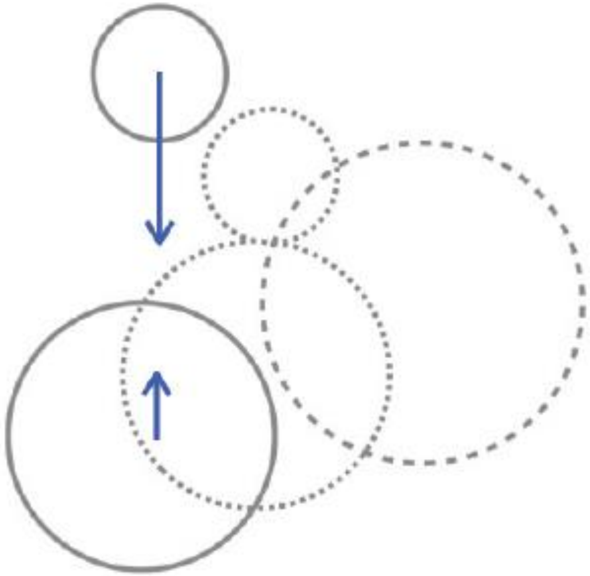

$$\bar{r}_\mathrm{b}^n \propto D_\mathrm{X} c_\mathrm{He} t$$

surface diffusion (sd), n=5-6
volume diffusion (vd)
vapor transport through the bubble (g)

Ostwald Ripening (dissociation)

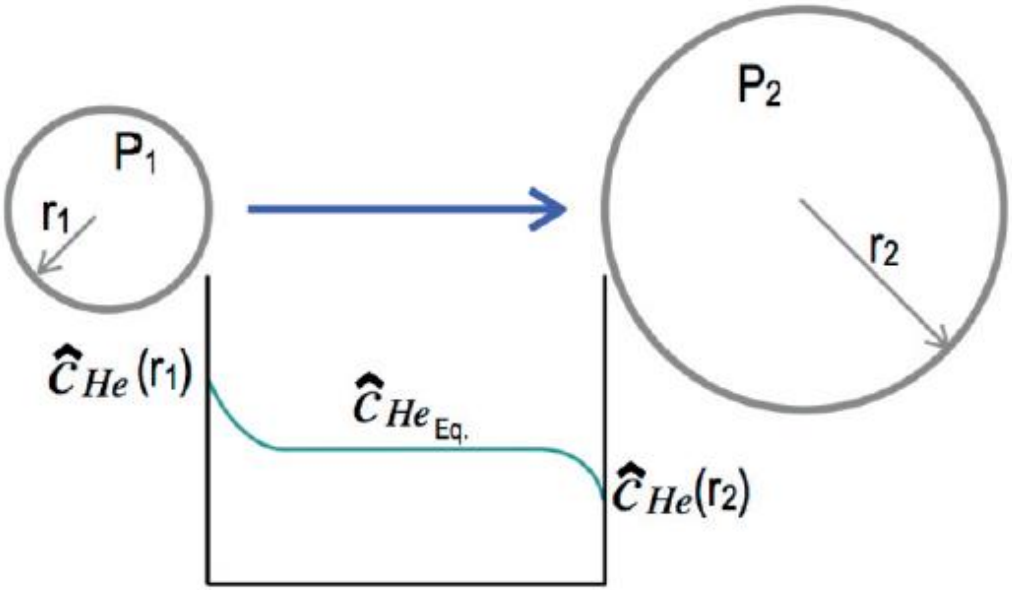

$\bar{r}_\mathrm{b}^2 \propto kTD_\mathrm{He}K_\mathrm{He}t$ Helium dissociation

$\bar{r}_\mathrm{b}^3 \propto (\gamma\Omega/kT)D_\mathrm{V}t$ Vacancy dissociation

Helium bubble evolution

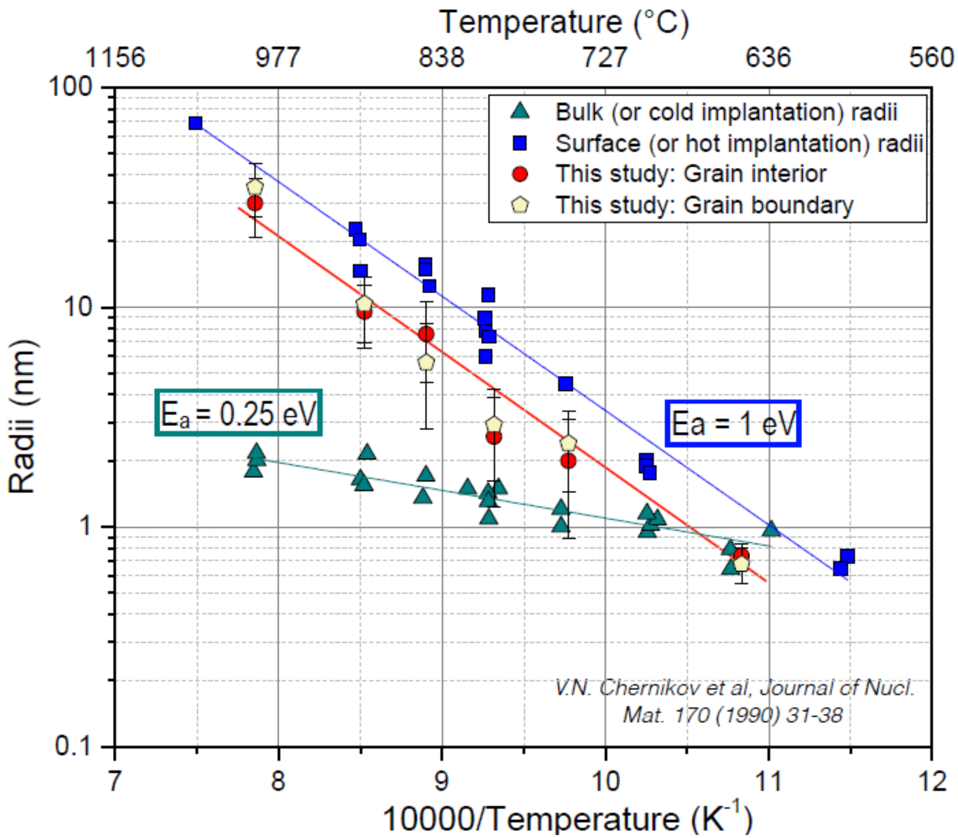

The thermal activation analysis shows that the He bubbles grow according to the **dissociative mechanism (Ostwald Ripening)** both, for GB and grain interior**.** This mechanism occurs **at least 300°C below** the one reported in RT implantation.

	Cold implant.	Hot implant.	Grain interior	Grain boundary
E_a (eV)	0.25	1.03	1.07	1.11
Q (eV, = $E_a n$)	1.26 - 1.51	2.06 – 3.07	2.14 – 3.21	2.22 – 3.33
Mechanism	Surf. diffusion	Dissociation	Dissociation	Dissociation

Contents

- Introduction
- Methodology
- Validation of miniaturized sample
- Bubble evolution after post He-implantation annealing
- Helium Hardening
- Helium effects on IASCC
- Summary, conclusions & perspectives

Helium bubble hardening

- **Models for YS increase**

1. DBH $\Delta\sigma_y = \alpha_i M \mu b (N_i d_i)^{1/2}$
2. FKH $\Delta\sigma_y = \alpha_i M \mu b r_i (N_i)^{2/3}$
3. BKS $\Delta\sigma_y = \alpha_i M \mu b (N_i d_i)^{1/2} \frac{1}{2\pi}\left[\ln\left(\frac{l}{b}\right)\right]^{-1/2}\left[\ln\left(\frac{D'}{b}\right)+0.7\right]^{3/2}$

α - hardening coefficient ≃ ?
M - Taylor factor ≃ 3
μ - shear modulus ≃ 76 GPa
b - Burgers vector ≃ 0.255 nm
N_i - Density of defects
d_i - diameter of defects
r_i - radius of defects
D' - Effective diameter

- **Tensile & microstructural data**

	1000 appm		300 appm		
	750°C	1000°C	750°C	850°C	950°C
Delta YS tensile (MPa)	123	24	45	37	29
AVG. Radii (nm)	1.8	27.5	1.4	3.9	17.6
AVG. Density (bubble/nm^3)	5.6×10^{-5}	1×10^{-7}	2.6×10^{-5}	1.6×10^{-6}	1×10^{-7}

We can determine the hardening coefficient (α)

DBH Model

$$\Delta\sigma_{y} = \alpha_i M \mu b (N_i d_i)^{1/2}$$

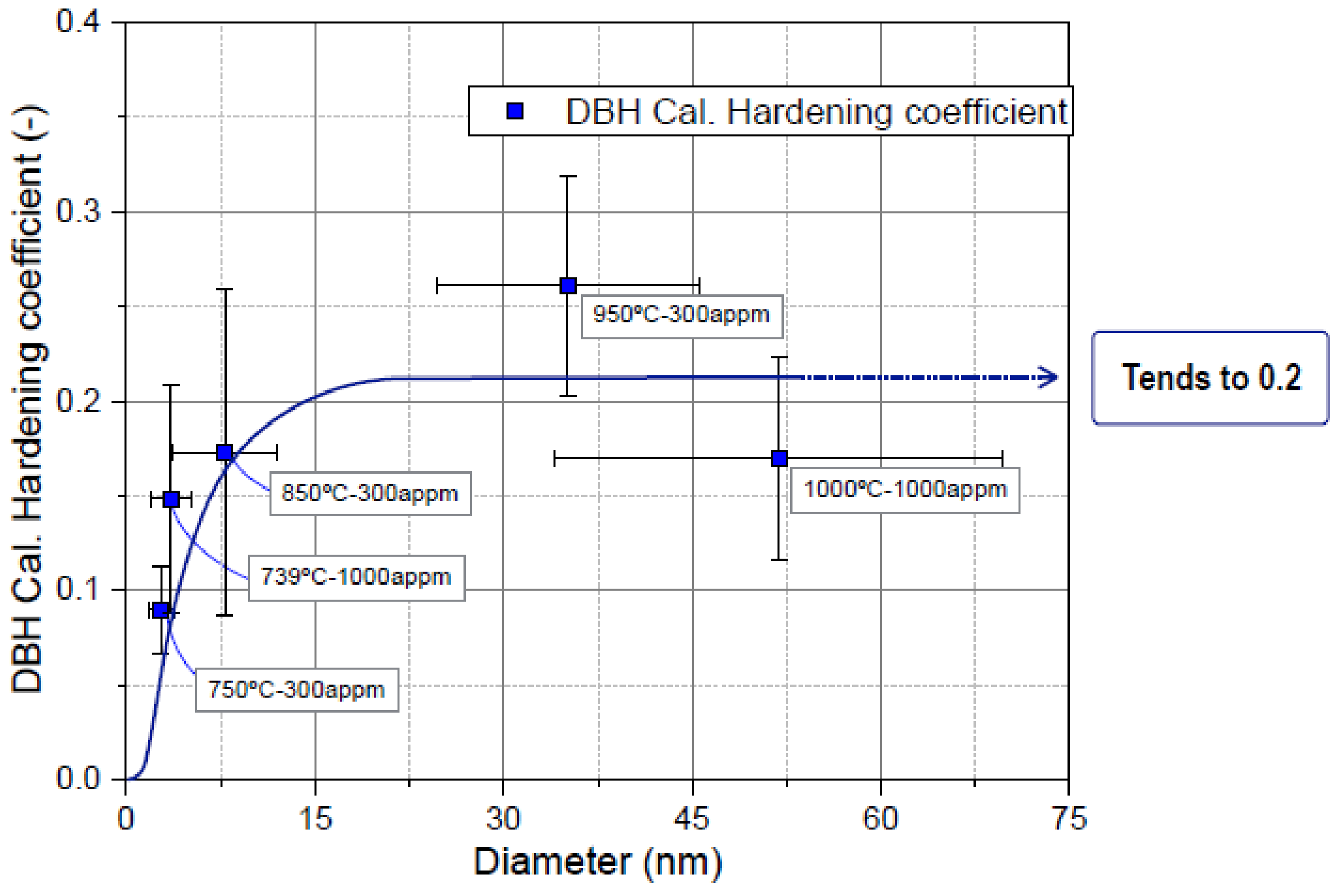

FKH Model

$$\Delta\sigma_y = \alpha_i M \mu b r_i (N_i)^{2/3}$$

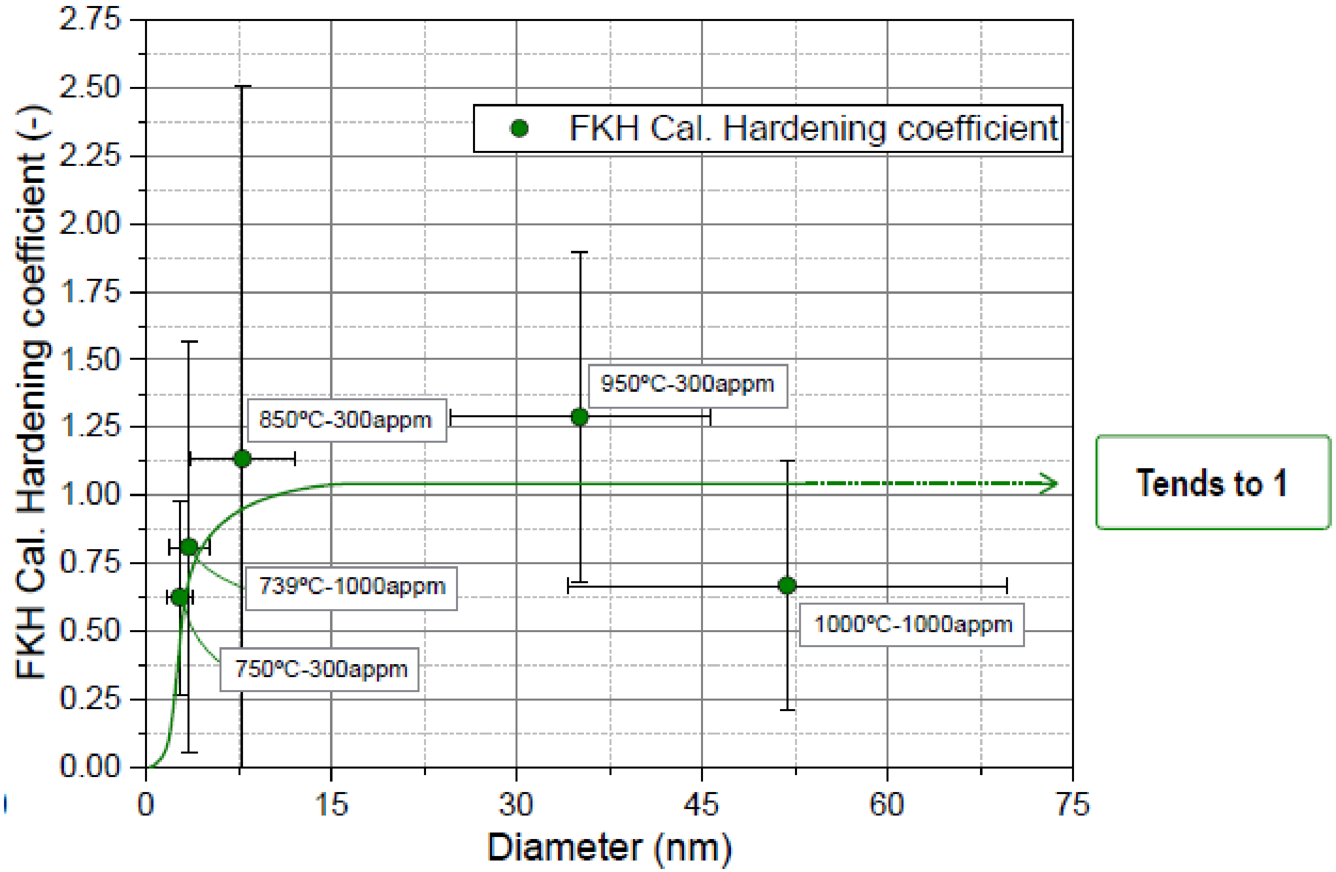

BKS Model

$$\Delta\sigma_y = \alpha_i M \mu b (N_i d_i)^{1/2} \frac{1}{2\pi}\left[\ln\left(\frac{l}{b}\right)\right]^{-1/2}\left[\ln\left(\frac{D'}{b}\right)+0.7\right]^{3/2}$$

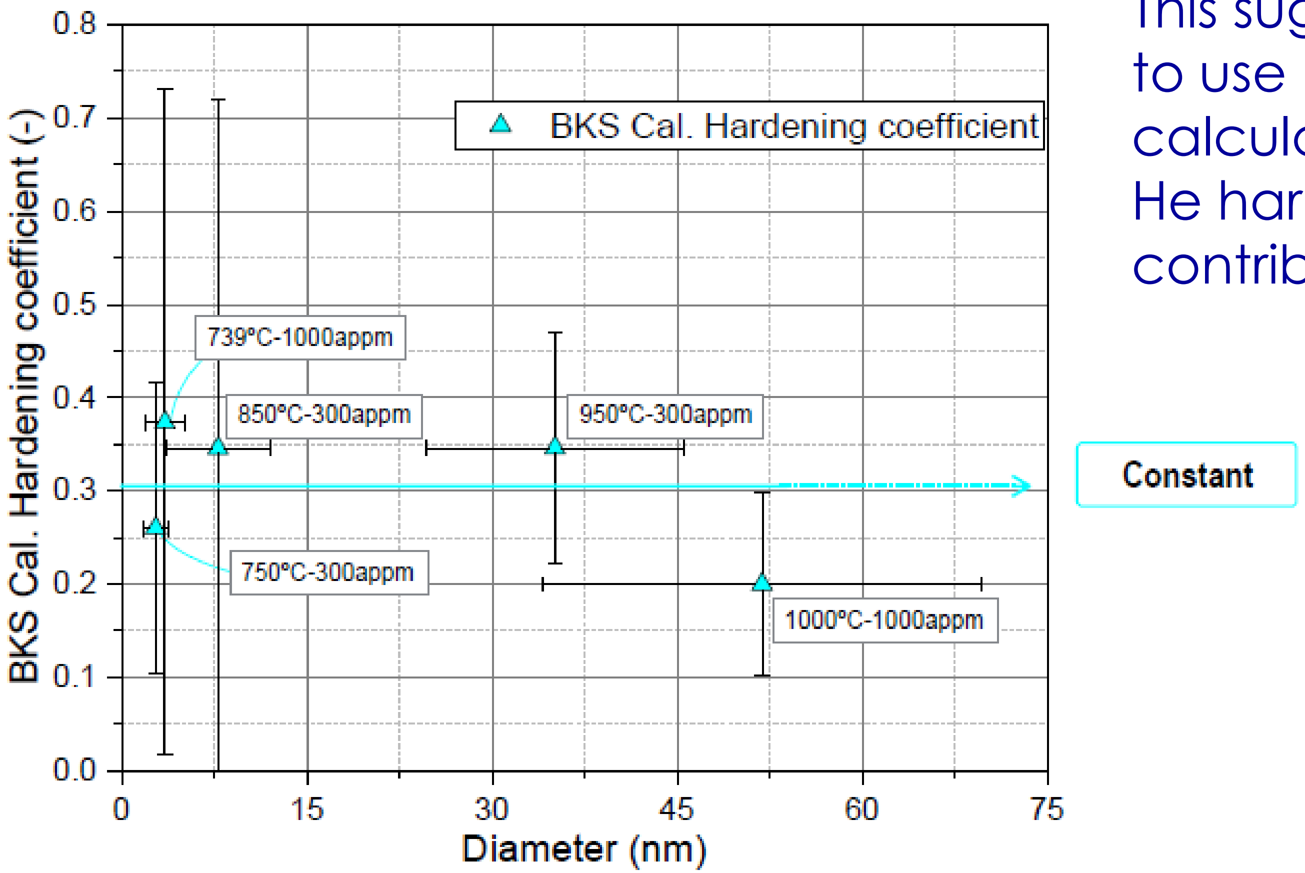

This suggests to use BKS for calculating the He hardening contribution

Contents

RIS on grain boundary

- GB RIS with FEI TALOS F200X (200 kV)

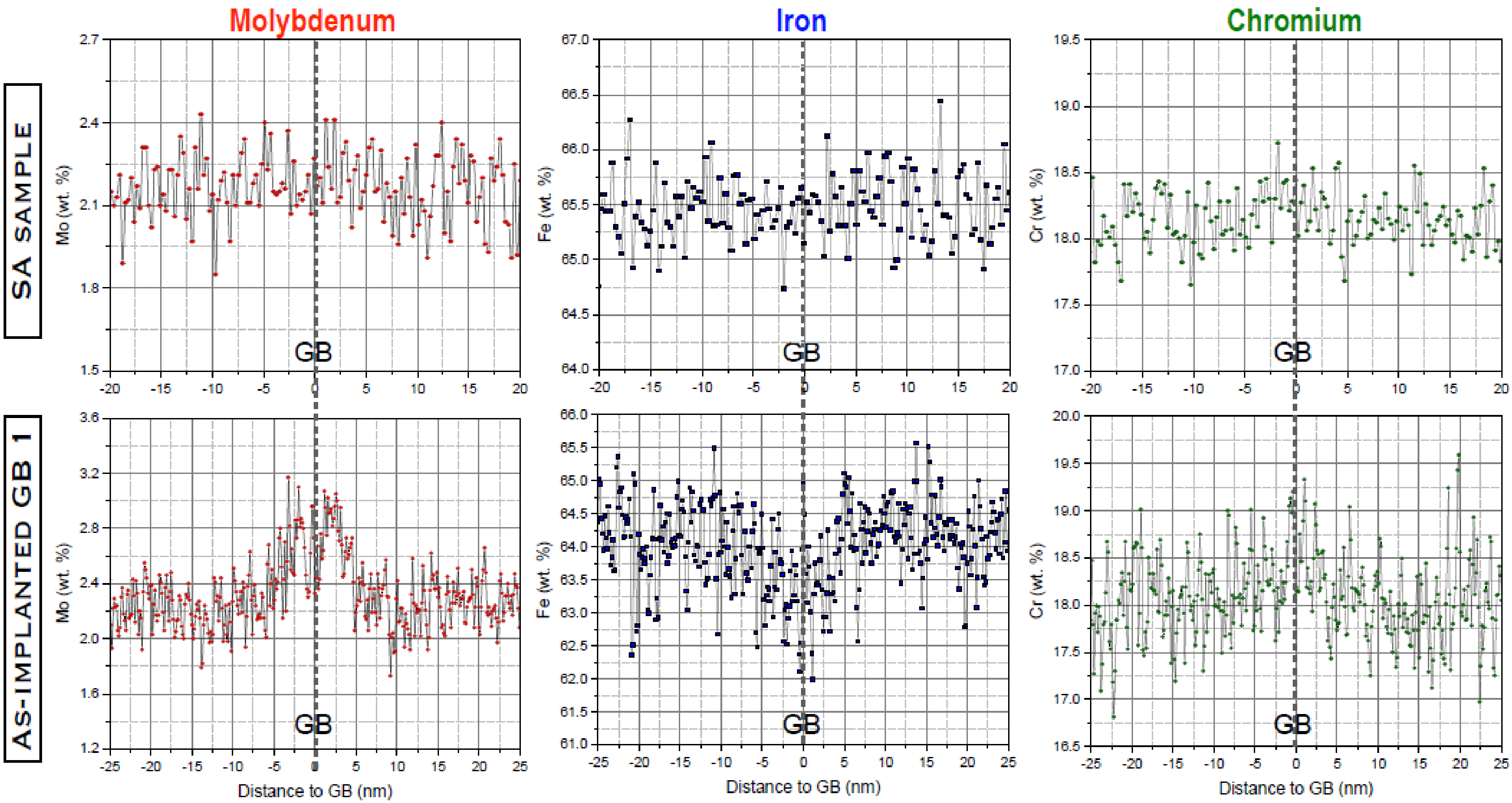

Enrichment
2.1⟶3 % wt.
Usually W shape

Depletion
64.5⟶63.5 % wt.
Usually V shape

No measurable effect

SSRT to SA + 1000 appm samples

- **1000 appm with/out HT**

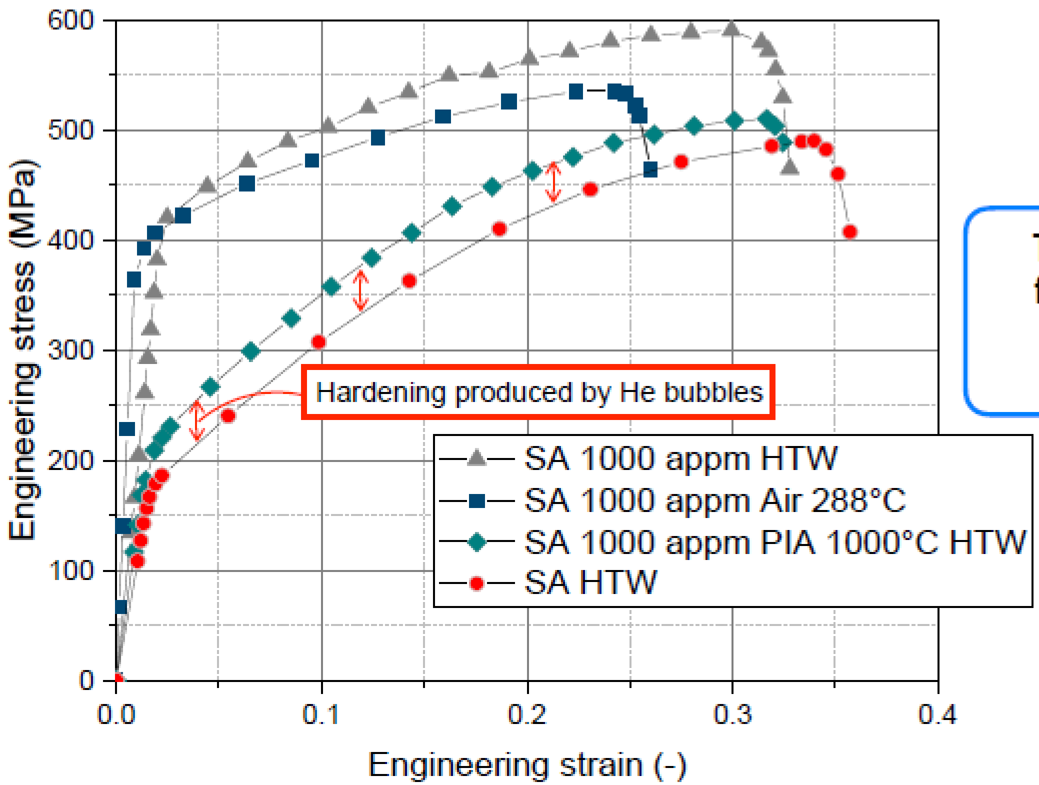

Transgranular dimple fracture is dominant, some transgranular cleavage in HTW

	SA HTW	1000appm Air 288°C	1000appm HTW	1000appm PIA 1000°C HTW
YS	178	383	418	198
UTS	492	547	594	513
ε_u (plastic)	0.28	0.23	0.26	0.27

SSRT to CW + 1000 appm samples

- **CW with/out 1000 appm**

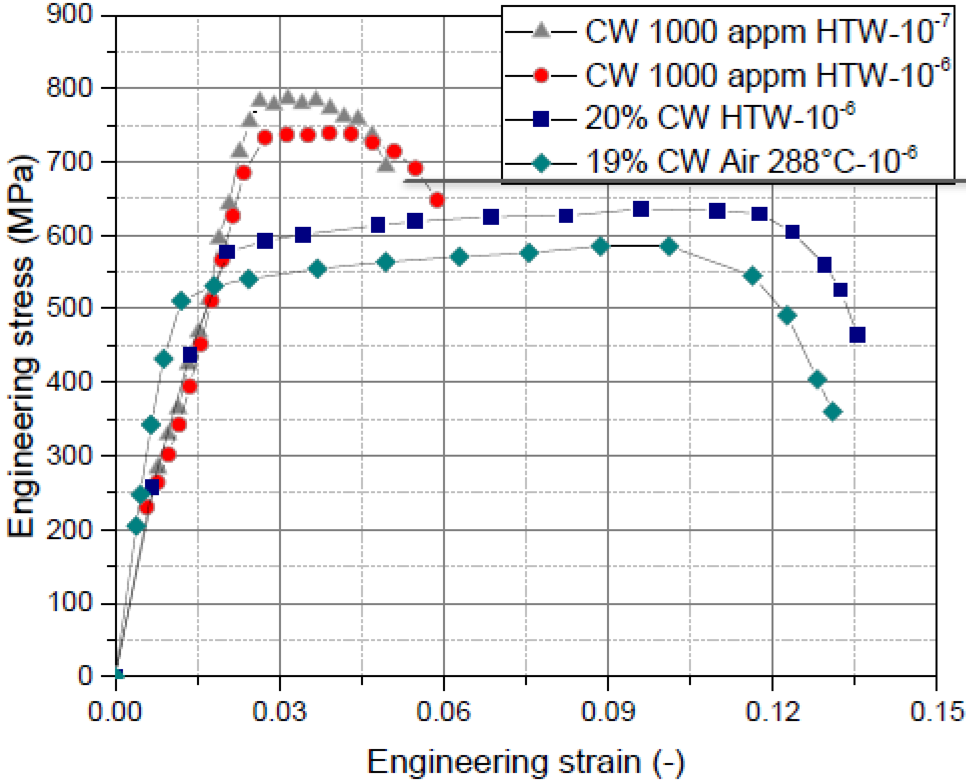

CW samples show tensile response similar to IASCC curves

Transgranular dimple fracture is dominant, some transgranular cleavage in HTW

	CW HTA	CW HTW	CW-1000appm	CW-1000appm 10^{-7}
YS	579	576	734	787
UTS	631	641	740	790
ε_u (plastic)	0.08	0.08	0.013	0.001

Metallography investigations

Surface of the samples tested in different environment and material conditions

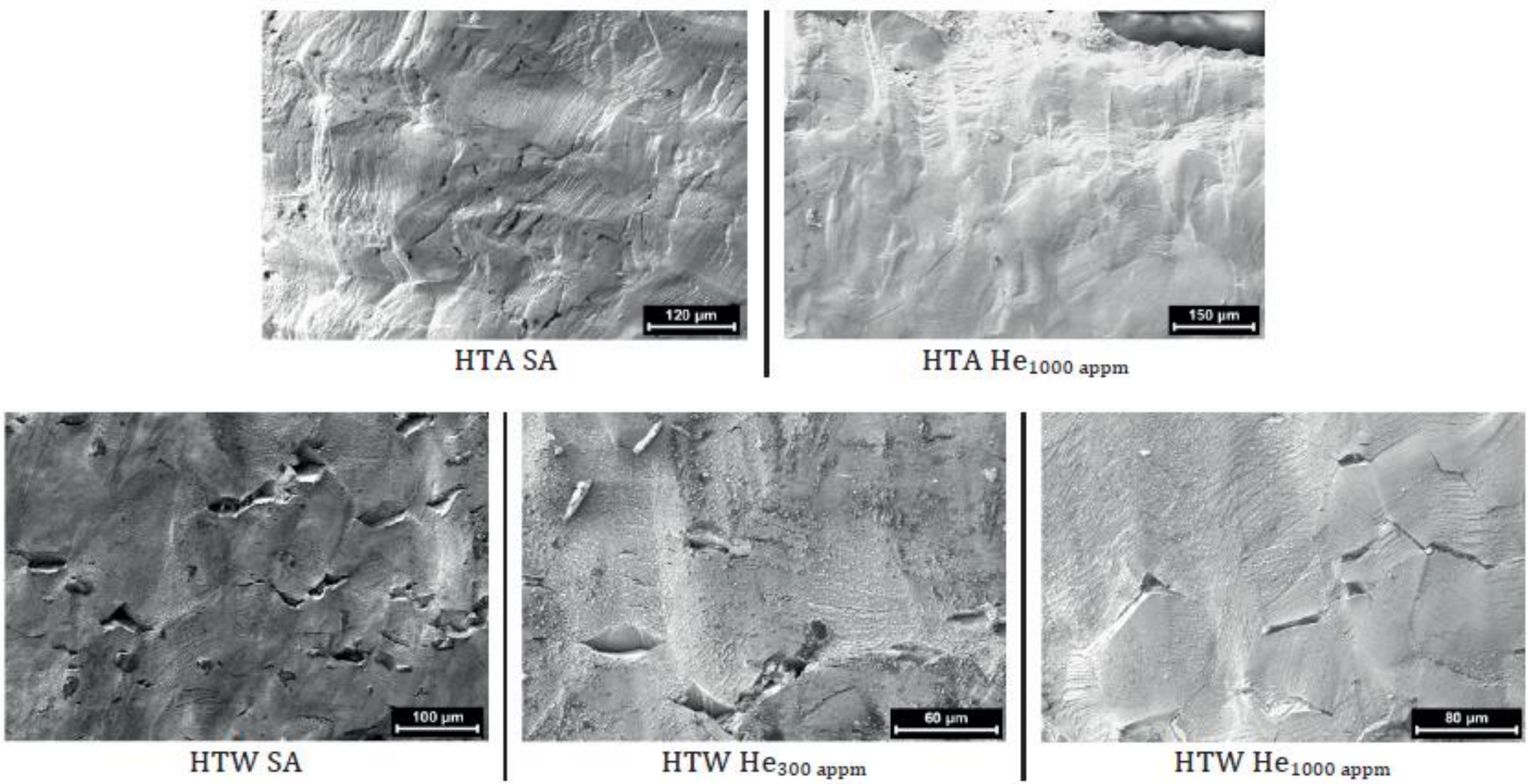

Fracture investigations

- **Fracture surface: 1000 appm with/out HT**

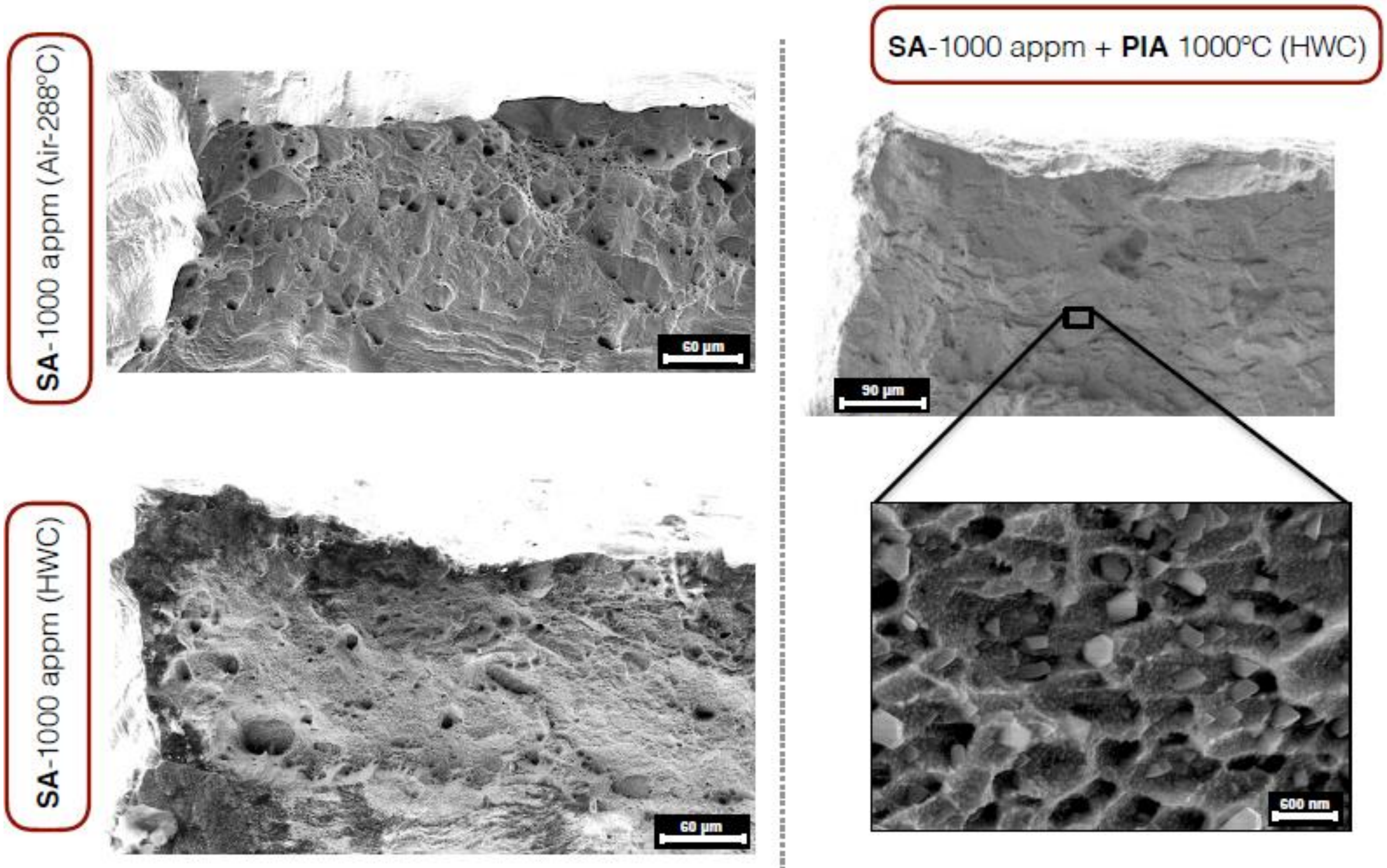

TEM investigation

- **Deformation microstructure (all HTW)**

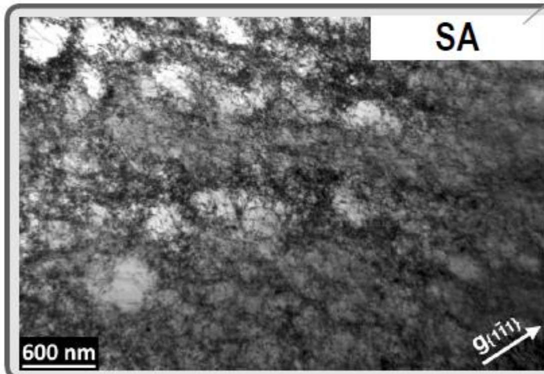

3D deformation cells typical for high Ni contents.

As-implanted samples

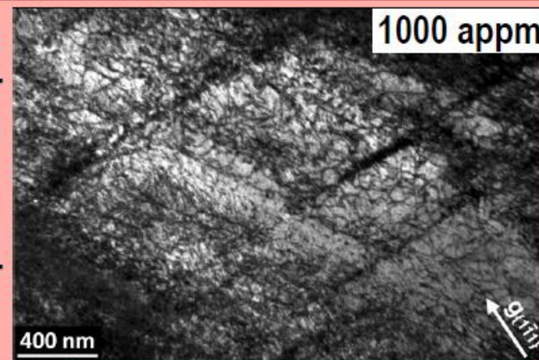

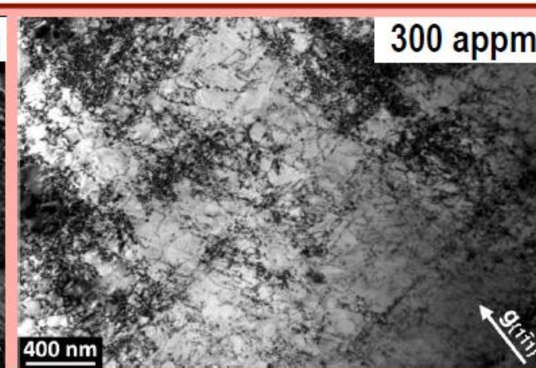

No apparent 3D deformation cells with random arrangement of dislocations. Microstructure that might be a precursor for SCC.

As-implanted CW

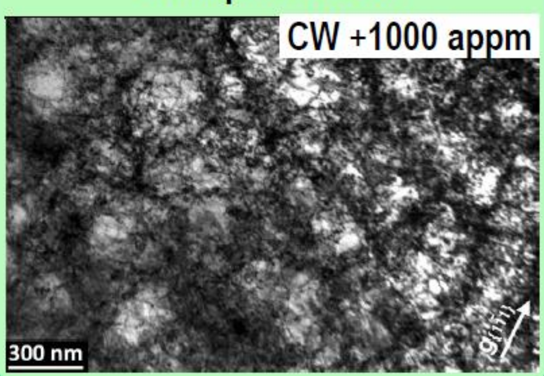

Prior 3D deformation microstructure still present. No evident increase of more planar deformation

Post-implantation annealed

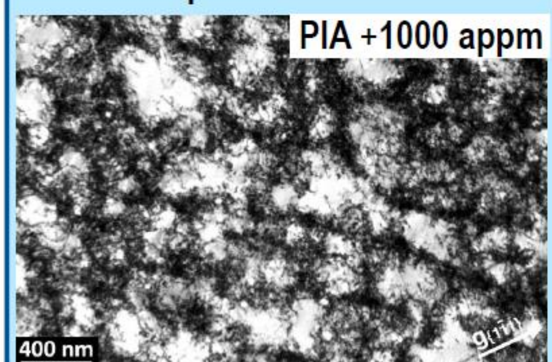

Recover 3D deformation microstructure

26

Discussion

- **Why don't we see IASCC?**

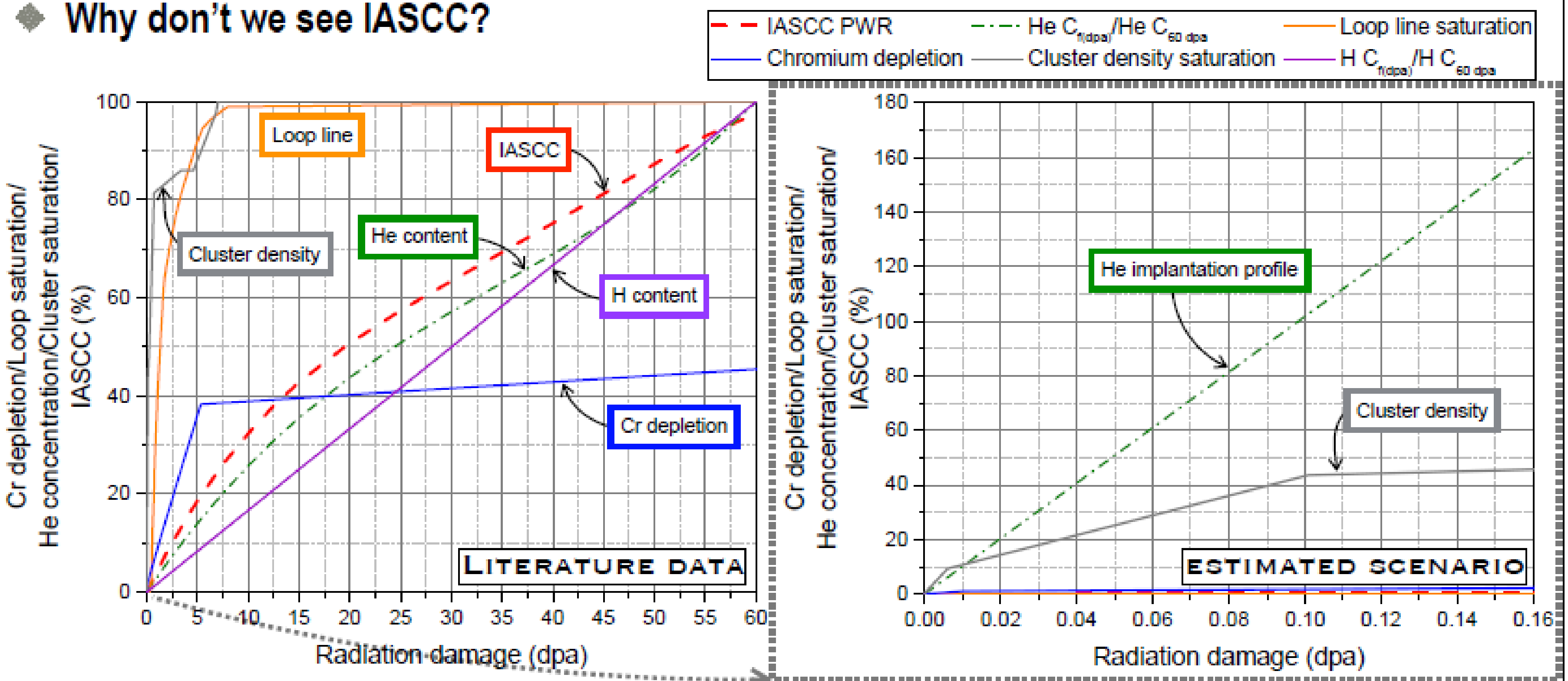

Main differences

- Chromium
- Black dots
- # of loops
- Hydrogen
- Hardening

Contents

Summary, conclusions & perspectives I

- Results of SSRT of 316L sample in air and different hot water (different chemical water conditions) for standard and miniaturized flat dog-bone samples show that the mechanical properties and fracture mode are almost identical for both sample types.
- Optical microscope and SEM observations show 100% ductile fracture mode after SSRT test for RT and HT in air, normal hot water conditions but 2% cleavage appearances at hydrogenated hot water condition (288°C)
- Similar bubble size & distance in grain interior and on GB. PIA increases bubble size, but does only moderately increase GB He bubble coverage.
- The activation energy of bubble evolution for GB and Matrix shows that in both cases the bubble grows with dissociative mechanism (OR). This mechanism occurs 300°C below the one reported in RT implantation. The coarsening mechanism might depend on both annealing T and bubble size.
- The hardening coefficient increases with the bubble size in the FKH and DBH models but not in BKS model. This suggests to use BKS for calculating the He hardening contribution.
- Homogenized He implantation in SA and CW at 300°C up to 1000 appm results in very limited RIS only (only Mo).

Summary, conclusions & perspectives II

- The deformation microstructure clearly changes from dislocation cells to random distribution of dislocations in SA & He implanted samples, respectively. The formation of deformation bands is enhanced in as-implanted condition.
- Accelerated SSRT (10^{-6} - 10^{-7} s^{-1}) in HTW with 2.2 ppm DH at 290 °C **did not induce IG(IA)SCC initiation** in smooth tensile specimens with homogenized helium implantation at 300°C up to 1000 appm (<0.16 dpa) in SA, CW and PIA (≤ 1000°C) conditions.
- However, the mechanically dominated short-term SSRT may be too short to exclude SCC initiation and could overlook other more time-consuming (e.g. corrosion-dominated) precursor and initiation processes.
- These results suggest that a helium concentration ≤1000 appm alone cannot induce IASCC, therefore there has to be **some synergy between irradiation damage and helium concentration.**
- The formation of irradiation-induced dislocation channels (at high dose) with high-stress concentration on grain boundaries, together with the current helium bubbles grain boundary coverage (~10%), could promote intergranular cracking.
- Further evaluations should thus include samples with high displacement damage (besides of high helium concentration) and crack growth experiments with pre-cracked specimens.

Acknowledgments

This work was supported by Euratom research and training program 2014-2018 under Grant Agreement No 661913 (SOTERIA) and Swissnuclear